ELSEVIER

Journal of Alloys and Compounds 262–263 (1997) 521–528

Journal of ALLOYS AND COMPOUNDS

Nitridation of Ti/Nb alloys and solid-state properties of δ-(Ti,Nb)N

W. Mayr[a], W. Lengauer[a,*], V. Buscaglia[b], J. Bauer[c], M. Bohn[d], M. Fialin[e]

[a] *Institute for Chemical Technology of Inorganic Materials, Vienna University of Technology, Getreidemarkt 9 / 161, A-1060 Vienna, Austria*

[b] *Istituto di Chimica Fisica Applicata dei Materiali, Consiglio Nazionale delle Ricerche, via de Marini 6, I-16149 Genoa, Italy*

[c] *Laboratoire du Chimie Solide et Inorganique Moléculaire, Université de Rennes I, Avenue Général Leclerc, F-35042 Rennes, France*

[d] *IFREMER, Centre de la Microsonde de l'Ouest, CNRS-UMR 6538, F-29280 Plouzané / Brest, France*

[e] *Centre d'Analyses par Microsonde CAMPARIS, Université P. et M. Curie, Tour 26 ét 3, 4, Place Jussieu, F-75252 Paris Cedex 05, France*

Abstract

The formation of microstructures and diffusion layers in the Ti-Nb-N system was investigated by annealing compact Ti/Nb alloys (0–100 at% Ti) in a high-purity nitrogen atmosphere (3 and 30 bar N_2) in the temperature range 1300–1600°C. The alloy starting material was in the form of wedge-type samples as well as in the form of plane sheets. After nitridation all samples showed a yellow colour which is characteristic for the fcc δ-(Ti,Nb)N phase, the layer growth rate of which was a minimum at 75 at% Ti. The nitride layer as well as the precipitates were rich in Ti whereas in the β alloy an Nb increase was observed. During nitridation needles with different length and width grew from the inner layer boundary into the original alloy. Electron probe microanalysis (EPMA) was performed to gain insight into the time evolution of the diffusion profiles of Ti, Nb and N. Homogeneous plane-sheet samples were used for measurements of the microhardness, the superconducting transition temperature and the lattice parameter of δ-(Ti,Nb)N. © 1997 Elsevier Science S.A.

Keywords: Layer growth; Microstructure; Diffusion couple; Superconductivity; EPMA; Microhardness; Lattice parameter

1. Introduction

The Ti-Nb-N system has been the subject of several previous investigations mostly because of the interesting superconducting behaviour of the δ-(Ti,Nb)N phase [1–7]. Pessall et al. [1,2] showed that the superconducting transition temperature reaches a maximum at TiN/NbN = 1.0 and obtained a value of 17.5 K (onset). As Ti/Nb alloys have a wide application as superconducting materials (T_c = 9.5 K [8]) a nitridation of these alloys is one possible technique to increase the T_c up to around 17 K. Since δ-(Ti,Nb)N is a brittle compound it is favourable to apply shaping operations on the Ti/Nb starting alloys and to perform a nitridation on the parts afterwards. One example of this is the production of superconducting r.f. cavities for particle accelerators [4,5]. Upon nitridation of Ti/Nb alloys diffusion of all components and layer formation occur.

The present work was carried out to investigate the diffusion of these compounds and the evaluation of microstructures as well as to measure some basic properties of δ-(Ti,Nb)N in order to obtain more insight needed for technical processes of fabrication and application of δ-(Ti,Nb)N-containing materials.

* Corresponding author. e-mail: wl@metec3.tuwien.ac.at

0925-8388/97/$17.00
PII S0925-8388(97)00367-8

2. Experimental

Seven different Ti/Nb alloys with a Ti content of 10, 25, 38, 50, 62, 75 and 90 at% Ti as well as the pure Ti and Nb metal were used as starting materials. The alloys were prepared from powder mixtures (Ti: Nisso, J, 99.7 wt% Ti; Nb: Goodfellow, GB, 99.85 wt% Nb) by arc melting. The specimens were homogenised at 1300°C under 100 mbar Ar atmosphere for at least 6 h and then cut into wedges. The nitridation was performed in a high-temperature autoclave with a tungsten heating element where the samples were annealed at 1300–1600°C in a high-purity nitrogen atmosphere under 3 and 30 bar N_2 (Table 1). The samples were cooled down to room temperature within a minute, then cut and embedded in cold-setting resin, ground (40-μm and 20-μm diamond disc) and polished (3-μm diamond paste and an aqueous SiO_2 suspension). Wedge-type samples were investigated by metallography for layer thicknesses and microstructures and subjected to EPMA [9]. The setup used for EPMA measurements is presented in Table 2. Homogeneous plane-sheet samples were investigated for Vickers microhardness as well as by X-ray powder diffraction. The N-content of the plane-sheet samples was analyzed by means of gas-chromatography (CHN 1108, Carlo Erba). For the electrical conductivity measurements bars of about 10 mm in length and 1 mm in width were cut from fully nitrided and homogeneous plane-sheet specimens and introduced into a double wall cryostat. The samples were cooled with liquid He down to 4.5 K. The electrical conductivity was measured in the temperature range 5–298 K. In addition, alloys with a Ti content of 25, 50 and 75 at% Ti were prepared from NbN (11.47 wt% N, 88.43 wt% Nb) and TiN (21.9 wt% N, 77.75 wt% Ti, 0.35 wt% O) by hot-pressing.

3. Results and discussion

3.1. Formation of diffusion layers and microstructural evaluation

In the system Ti-Nb-N all alloys formed a yellow coloured fcc δ-(Ti,Nb)N layer the thickness of which depends on the Ti/Nb ratio, the nitrogen pressure and the reaction temperature, respectively. It was found that the lower the nitrogen pressure the smaller the δ-phase band. This result corresponds to the findings of Martinelli [13], who reported thin layer thicknesses (Ti/Nb ratio = 63/37: 5–6 μm, Ti/Nb ratio = 54/46: 12–13 μm) at 0.3 bar N_2 and 1600°C for a reaction time of 12.0 h. In the case of wedge-type specimens, small sample thicknesses represent conditions after long- and thick sample thicknesses after short-annealing time [10]. Therefore the thickness of the δ-phase band was determined at different sample thicknesses to gain insight into the layer thickness

Table 1
Reaction conditions for partially and fully nitrided Ti/Nb alloys (HP, hot isostatic pressed)

Experiment	Composition (at% Ti)	Geometry	t (h)	T (°C)	p (bar N_2)
088	75,50,38,25	Plane-sheet	360.3	1650 ± 8	30.0 ± 0.1
111	100,90,62,10,0	Plane-sheet	124.3	1612 ± 6	30.0 ± 0.1
059	100,90,62,10,0	Wedge-type	8.0	1599 ± 10	29.9 ± 0.2
060	100,90,62,10,0	Wedge-type	49.7	1457 ± 9	29.6 ± 0.6
087	75,50,38,25	Wedge-type	50.3	1449 ± 9	29.6 ± 0.5
093	100,90,75,62,0	Wedge-type	8.3	1603 ± 5	3.1 ± 0.2
094	50,25,38,25,10	Wedge-type	8.1	1605 ± 8	3.0 ± 0.1
096	75,50,38,25	Wedge-type	7.9	1597 ± 6	30.0 ± 0.1
101	100,90,62,10	Wedge-type	306.8	1297 ± 9	30.0 ± 0.1
107	75,50,38,25,0	Wedge-type	309.8	1299 ± 6	29.9 ± 0.2
HP	75,50,25	Plane-sheet	360.3	1650 ± 8	30.0 ± 0.1

Table 2
EPMA setup for the system Ti-Nb-N

Element	Crystal	Peak-position [$10^5 \times \sin\Theta$]	+bg. shift [$10^5 \times \sin\Theta$]	−bg. shift [$10^5 \times \sin\Theta$]	bg. slope [$10^5 \times \sin\Theta$]	t (s)	Count-rate (c/snA)	σ (c/snA)
Ti	PET	31394	600	—	1.2	6	196.79	0.3
Nb	PET	65423	2200	1450	0.0	6	66.23	0.5
N	PC1	52932	5000	4500	0.0	6	13.61	1.1

Acceleration voltage: Nb, Ti, 10 kV; N, 5 kV.
Beam current: Nb, Ti, N, 100 nA.

Table 3
Layer thickness (d) of δ-(Ti,Nb)N as a function of the nitrogen pressure as well as of the sample thickness

Composition/sample thickness	T = 1600°C, p = 30.0 bar N_2			T = 1600°C, p = 3.0 bar N_2		
	800 μm d (μm)	1200 μm d (μm)	1600 μm d (μm)	800 μm d (μm)	1200 μm d (μm)	1600 μm d (μm)
Ti	800	353	235	800	470	320
$Ti_{0.90}Nb_{0.10}$	157	137	118	152	127	117
$Ti_{0.75}Nb_{0.25}$	69	29	25	20	15	15
$Ti_{0.62}Nb_{0.38}$	72	49	39	59	39	29
$Ti_{0.50}Nb_{0.50}$	78	49	25	56	39	29
$Ti_{0.38}Nb_{0.62}$	118	93	59	78	68	55
$Ti_{0.25}Nb_{0.75}$	157	132	69	117	88	79
$Ti_{0.10}Nb_{0.90}$	167	146	118	127	98	92
Nb	196	176	167	147	141	151

enlargement (Table 3). In Figs. 1a–g microstructures of the different nitrided Ti/Nb alloys are shown. It is clearly visible that needles with different shapes grew from the inner layer boundary of the δ-phase into the base alloy. An important result is that the higher the Nb content the smaller are the needles and the precipitates (Figs. 1a–g).

EPMA measurements were difficult to perform in Nb-rich samples since nitride precipitates were in the same order of magnitude as the lateral resolution of the technique (≤ 5 μm). EPMA line scans across different Ti-Nb-N diffusion couples are shown in Figs. 2a–e. In the case of the sample 060, 90 at% Ti (Fig. 1a, Figs. 2a–c) the nitride layer as well as the N-rich precipitates consisted of δ-(Ti,Nb)N whereas in the N-poor regions of the sample the precipitates consisted of α-(Ti,Nb)(N). The formed nitrides are richer in Ti than the starting alloys whereas the remaining alloy showed an Nb enrichment. The reason for this result is the higher affinity of Ti versus N as compared to that of Nb. In Fig. 2d (compare microstructure Fig. 1c) the EPMA scan of the sample 060, 62 at% Ti is presented. The thin nitride layer as well as the nitride precipitates consisted of δ-(Ti,Nb)N. Six different curves can be observed in the EPMA scan (Fig. 2d). Three of them represent the concentrations of the compounds in the alloy and the nitride, respectively. The Nb enrichment in the alloy near the surface is clearly visible. In Fig. 2e (compare microstructure Fig. 1g) the EPMA scan of sample 060, 10 at% Ti is shown. In contrast to Ti-rich alloys the nitride precipitation consisted of β-$(Ti,Nb)_2N$. The typical composition of the nitrides and the alloy as obtained by EPMA investigations are given in Table 4.

3.2. Diffusion behaviour in the Ti-Nb-N system

In order to observe the diffusion path upon diffusion of different Ti/Nb alloys, the EPMA data were introduced into a triangle diagram (Fig. 3). In the case of the sample 060, with a Ti-content of 90 at% Ti, three phases were observed δ-(Ti,Nb)N, α-Ti(Nb,N) and β-(Ti,Nb) whereas in the sample 060 (Ti = 10 at% Ti) δ-(Ti,Nb)N, β-$(Ti,Nb)_2N$ and β-(Ti,Nb) were obtained. In those regions of the Ti-rich samples (Ti = 38–90 at% Ti) where nitrogen saturation is finished α-(Ti,Nb)(N) is obtained with a Ti content higher than the starting alloys while β-(Ti,Nb) shows a slight increase in Nb. In samples with a Ti content of Ti ≤ 25 at% Ti, at the surface a δ-(Ti,Nb)N layer is formed while the precipitates consisted of β-$(Ti,Nb)_2N$. In Ti-rich samples the nitrogen concentration increases and α-(Ti,Nb)(N) is converted into δ-(Ti,Nb)N. In Nb-rich specimens β-$(Ti,Nb)_2N$ is formed and subsequently transformed into δ-(Ti,Nb)N. In the δ-phase the Ti/Nb ratio is shifted to higher Ti values. Therefore in the final stage of nitridation Ti and Nb diffusion has to occur over quite long distances for homogenisation of the sample. Interestingly, this homogenisation is quite fast (e.g. in contrast to the Ti-Zr-N system [11]) in view of the usual high activation energy of metal diffusion (causing generally a low diffusion rate).

3.3. Solid-state properties

Due to the fast homogenisation of components in nitrided Ti/Nb alloys, plane sheets were prepared (T = 1650°C, p = 30.0 bar N_2, t = 360.3 h) leading to homogeneous δ-(Ti,Nb)N (proved by EPMA) and a variety of solid-state properties could be measured. The lattice parameter of the fcc δ-(Ti,Nb)N phase depends on the Ti/Nb ratio as well as on the nitrogen content of the specimens. The values are given in Table 5 and presented in Fig. 4. A slight positive deviation of the lattice parameter can be observed in samples with a Ti content between 0 and 75 at% Ti. Both Ti-rich samples with a Ti content of 90 and 100 at% Ti are situated below the mean value. This is because the N content of both specimens is about 46 at% N. The lattice parameter of sub-stoichiometric δ-TiN is lower as compared to stoichiometric δ-TiN

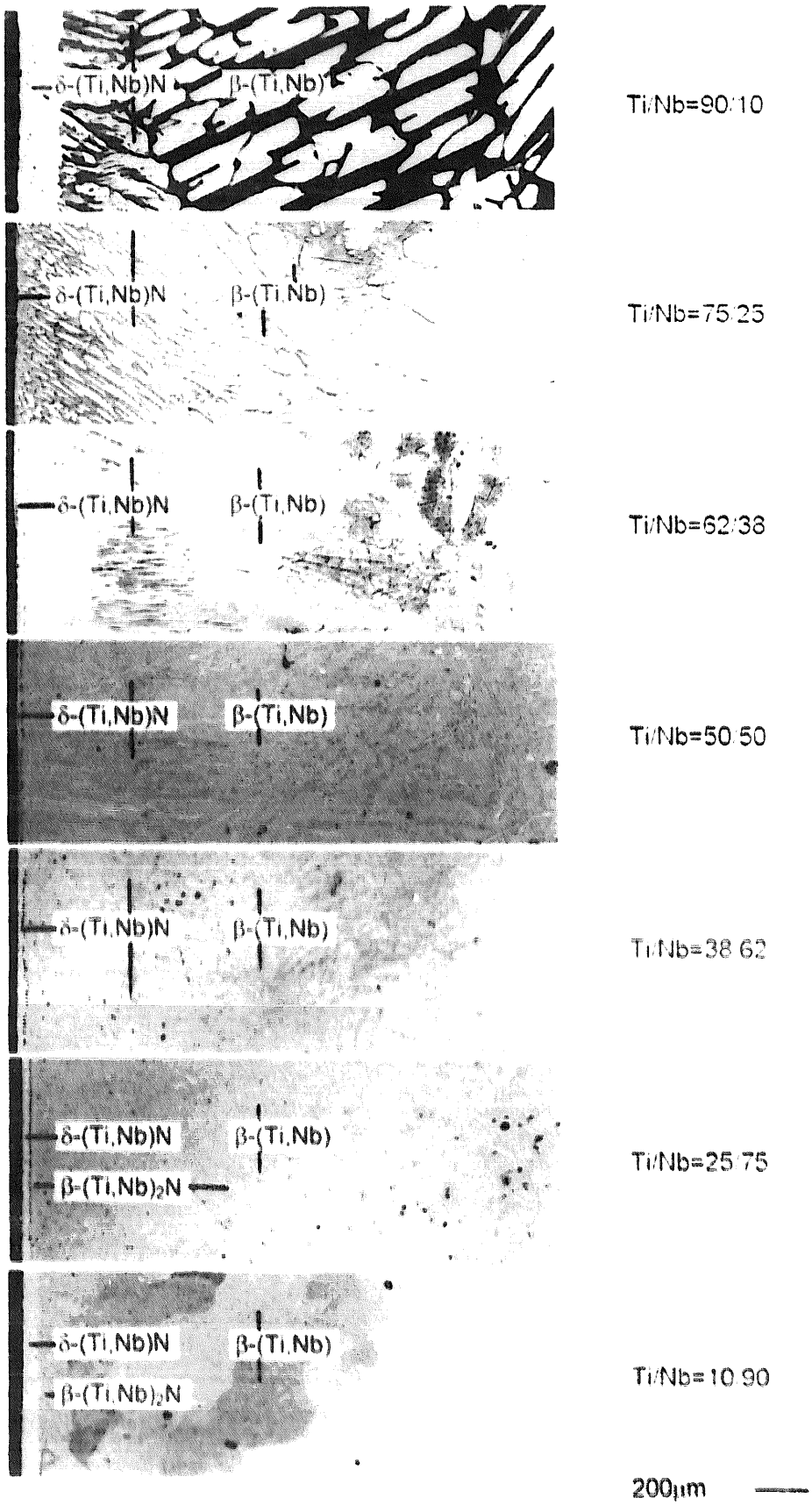

Fig. 1. Microstructures of Ti-Nb-N diffusion couples. (a) 060 (T = 1457°C, p = 29.6 bar N_2, t = 49.7 h), Ti = 90 at% Ti; (b) 087 (T = 1449°C, p = 29.6 bar N_2, t = 50.25 h), Ti = 75 at% Ti; (c) 060, Ti = 62 at% Ti; (d) 087, Ti = 50 at% Ti; (e) 087, Ti = 38 at% Ti; (f) 087, Ti = 25 at% Ti and (g) 060, Ti = 10 at% Ti.

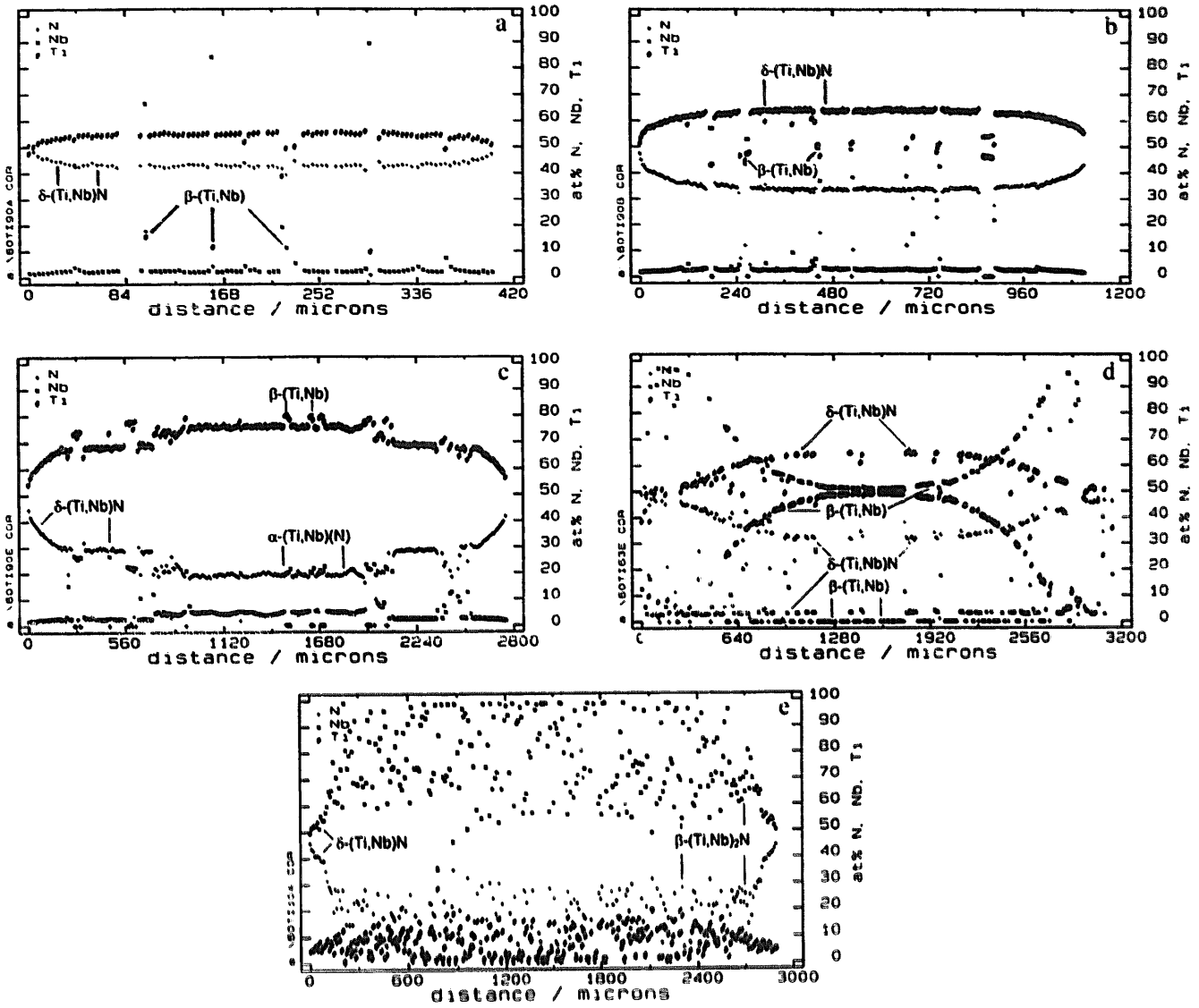

Fig. 2. (a) Nitrogen, titanium and niobium profiles in a wedge-type Ti-Nb-N diffusion couple (060, [Ti]/[Nb] = 90/10, T = 1457°C, p = 29.6 bar N_2, t = 49.7 h, sample thickness: 400 μm). (b) Nitrogen, titanium and niobium profiles in a wedge-type Ti-Nb-N diffusion couple (060, [Ti]/[Nb] = 90/10, T = 1457°C, p = 29.6 bar N_2, t = 49.7 h, sample thickness: 1100 μm). (c) Nitrogen, titanium and niobium profiles in a wedge-type Ti-Nb-N diffusion couple (060, [Ti]/[Nb] = 90/10, T = 1457°C, p = 29.6 bar N_2, t = 49.7 h, sample thickness: 2750 μm). (d) Nitrogen, titanium and niobium profiles in a wedge-type Ti-Nb-N diffusion couple (060, [Ti]/[Nb] = 62/38, T = 1457°C, p = 29.6 bar N_2, t = 49.7 h, sample thickness: 3150 μm). (e) Nitrogen, titanium and niobium profiles in a wedge-type Ti-Nb-N diffusion couple (060, [Ti]/[Nb] = 10/90, T = 1457°C, p = 29.6 bar N_2, t = 49.7 h, sample thickness: 2900 μm).

[12]. Martinelli [13] also measured lattice parameters of different Ti/Nb alloys. However, the specimens were annealed at a maximum nitrogen pressure of 300 mbar N_2. Therefore nitrogen concentration on the sample surface during nitridation was lower compared to our experiments, thus leading to smaller nitrogen concentrations in the samples especially at higher Nb contents. The obtained data of microhardness (H_V) are given in Table 5. The values show a slight increase with increasing Ti content (Fig. 5). The nitrogen concentration especially of the binary specimens TiN and NbN is lower than those of Ti/Nb alloys. As the microhardness is dependent on the nitrogen content, literature data of stoichiometric compounds [10,12,14] were included in Fig. 5 too.

The superconducting transition temperature as determined by four-point measurements shows a strong dependency upon the Ti/Nb ratio as well as on the nitrogen content (Table 5, Fig. 6). The transition temperature of $NbN_{0.71}$ is about 0.49 K lower compared to the one of $NbN_{0.99}$. The ternary alloys show a slight increase of the transition temperature with increasing Ti content. The maximum (17.13 K) is reached at a Ti/Nb ratio of 50/50. Compared to the values of Pessall et al. [1,2] the T_C values show the same dependency on the Ti/Nb ratio and reach a

Table 4
Composition of phases in the partially nitrided alloys

Experiment/designation	Phase	N (at% N)	Ti (at% Ti)	Nb (at% Nb)
060	δ-(Ti,Nb)N	44.4–29.1	56.4–68.5	1.6–2.5
$Ti_{0.90}Nb_{0.10}N$	α-(Ti,Nb)(N)	18.8	76.0	4.7
	β-(Ti,Nb)	2.6–0.0	72.0–79.6	25.4–20.4
087	δ-(Ti,Nb)N	46.8–34.7	50.0–62.2	3.2–3.1
$Ti_{0.75}Nb_{0.25}N$	β-(Ti,Nb)	0	3.6–43.8	96.4–56.2
060	δ-(Ti,Nb)N	47.8–31.7	49.1–64.6	3.1–3.7
$Ti_{0.62}Nb_{0.38}N$	β-(Ti,Nb)	0	3.1–49.1	97.0–50.9
087	δ-(Ti,Nb)N	47.7–38.6	47.8–58.1	4.5–3.3
$Ti_{0.50}Nb_{0.50}N$	β-(Ti,Nb)	16.1–0.7–0.0	8.3–3.5–18.3	75.6–95.8–81.73
087	δ-(Ti,Nb)N	47.3–42.7	46.2–53.9	6.5–3.4
$Ti_{0.38}Nb_{0.62}N$	β-(Ti,Nb)	5.4–0.0–0.0	7.2–2.3–6.7	87.4–97.7–93.3
087	δ-(Ti,Nb)N	44.0–26.5	13.9–10.7	42.1–62.9
$Ti_{0.25}Nb_{0.75}N$	β-$(Ti,Nb)_2N$	26.5–24.1	10.7–12.3	62.9–63.6
	β-(Ti,Nb)	0	2.0–2.1	98.0–97.9
060	δ-(Ti,Nb)N	45.7–38.9	4.8–6.7	49.5–54.4
$Ti_{0.10}Nb_{0.90}N$	β-$(Ti,Nb)_2N$	31.5–22.7	8.9–13.2	59.6–64.1
	β-(Ti,Nb)	0	0.9–1.4	99.1–98.6

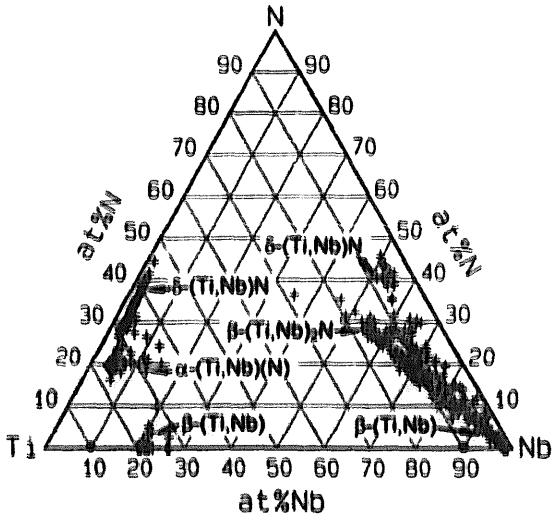

Fig. 3. Triangle diagram with data from EPMA scans at large sample thicknesses (060, $Ti_{0.90}Nb_{0.10}N$ and $Ti_{0.10}Nb_{0.90}N$, T = 1457°C, p = 29.6 bar N_2, t = 49.7 h).

maximum at the same composition. As can be seen in Fig. 6 only the hot-pressed sample with a composition of Ti/Nb = 1 reaches this value. Between 50–90 at% Ti the T_c values decrease steeply. Buscaglia et al. [5] measured the transition temperature by ac susceptibility as a function of temperature. A broad maximum of the critical transition temperature was obtained between 30 and 60 at% Ti. The reaction pressure in their experiments was about 0.15 bar N_2 leading to a different nitrogen content in the samples as compared to the present study.

4. Conclusion

Nitridation of Ti/Nb alloys was studied in the temperature range 1300–1600°C under high-purity nitrogen atmosphere (3 and 30 bar N_2) for times ranging from 8 to 360 h. The experiments led to the following conclusions.

All alloys formed a yellow coloured fcc δ-(Ti,Nb)N phase band, the layer growth rate of which showed a dependency on the Ti/Nb ratio as well as on the nitrogen pressure. A minimum was obtained at 75 at% Ti. The higher the Nb content of the alloy is, the smaller are the needles and the precipitates being formed during nitridation. In the case of the sample with a Ti content of 90 at% Ti three phases were observed δ-(Ti,Nb)N, α-(Ti,Nb)(N) and β-(Ti,Nb) whereas in specimens with a Ti content between 38–75 at% Ti only δ-(Ti,Nb)N and β-(Ti,Nb) were obtained. In Nb-rich samples (Ti = 10–25 at% Ti) δ-(Ti,Nb)N, β-$(Ti,Nb)_2N$ and β-(Ti,Nb) were observed. Since Ti is nitrided first, the precipitates and nitride layer were found to be Ti richer than the starting alloys while β-(Ti,Nb) showed a slight increase in Nb.

The lattice parameter of alloys with a Ti content between 10–62 at% Ti showed a slight positive deviation from Vegards rule whereas the values of the Ti-rich samples are situated below the mean value. The obtained data of microhardness (H_V) showed a slight increase with increasing Ti content. The superconducting transition temperature showed a strong dependency upon the Ti/Nb ratio as well as on the

Table 5
Data on δ-(Ti,Nb)N

Sample/designation	N-content (at% N)	H_V (GPa)	T_C (ΔT) (K)	a (Å)
EQ18-1	41.7	13.7 ± 0.6	16.10(0.48)	4.3679(15)
EQ14-30	49.7	10.9 ± 0.5	16.59(0.18)	4.3921(2)
111NbN	47.6	—		4.3900(2)
$111Ti_{0.10}Nb_{0.90}N$	46.9	—	16.44(0.14)	4.3806(1)
$088Ti_{0.25}Nb_{0.75}N$	48.7	13.8 ± 0.7	16.60(0.34)	4.3603(1)
$HPTi_{0.25}Nb_{0.75}N$	48.1	—	—	4.3652(23)
$088Ti_{0.38}Nb_{0.62}N$	48.8	14.2 ± 1.2	16.86(0.50)	4.3438(1)
$088Ti_{0.50}Nb_{0.50}N$	48.8	15.5 ± 1.0	11.16(0.36)	4.3260(1)
$HPTi_{0.50}Nb_{0.50}N$	48.2	—	17.13(0.30)	4.3268(8)
$111Ti_{0.62}Nb_{0.38}N$	46.9	—	16.40(0.60)	4.3331(39)
$088Ti_{0.75}Nb_{0.25}N$	48.2	15.7 ± 1.5	13.68(1.20)	4.2881(3)
$HPTi_{0.75}Nb_{0.25}N$	49.3	—	—	4.2908(20)
$111Ti_{0.90}Nb_{0.10}N$	46.0	—	7.39(0.78)	4.2487(2)
111TiN	46.2	—	5.23(1.56)	4.2363(2)
TiN45	49.5	19.0 ± 0.8	—	—
TiN13	40.1	21.6 ± 2.2	—	—

H_V, Vickers microharness at a load of 0.98 N; T_C, four-point measurements, midpoint of 10/90% transition of conductivity; ΔT, temperature interval of 10/90% transition of the conductivity; a, lattice parameter (standard deviation in the last digits in parentheses).

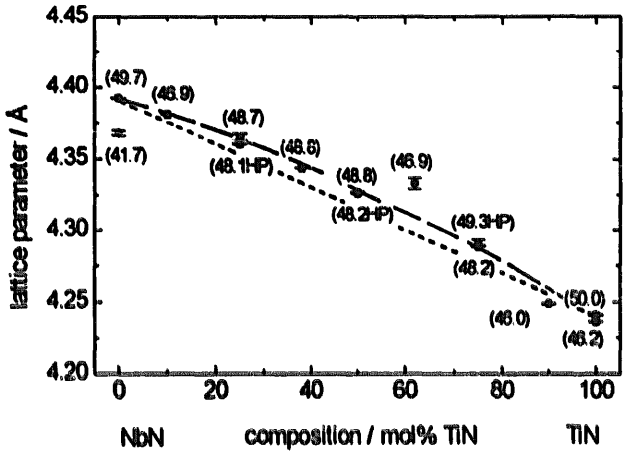

Fig. 4. Lattice parameter of the δ-(Ti,Nb)N phase as a function of composition (HP, hot-pressed; nitrogen content in parentheses).

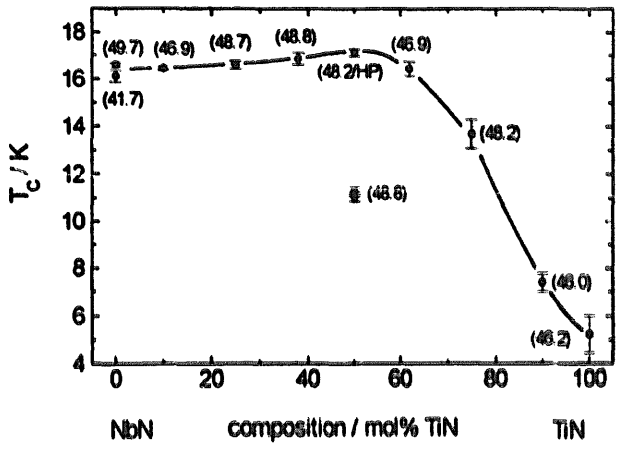

Fig. 6. Superconducting transition temperature of the δ-(Ti,Nb)N phase as a function of composition (HP, hot-pressed; nitrogen content in parentheses).

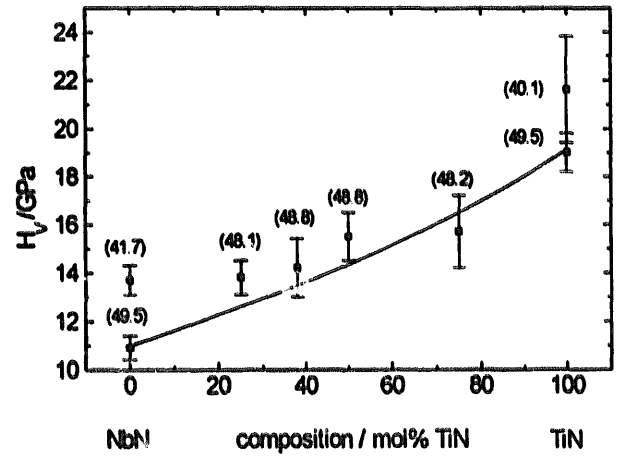

Fig. 5. Microhardness of the δ-(Ti,Nb)N phase as a function of composition (nitrogen content in parentheses).

nitrogen content. The T_C values showed a slight increase with increasing Ti content. The maximum (17.13 K) is reached at a Ti/Nb ratio of 50/50. Between 50–90 at% Ti the T_C data decrease steeply.

Acknowledgements

This project was supported by the Jubiläumsfonds der Oesterreichischen Nationalbank under project no. 5414 and the Austrian Academy of Sciences (ÖAW) under the project no. PICS-134. Dr. E. Bauer, Institute of Experimental Physics, TU Vienna, made electrical conductivity measurements possible.

References

[1] N. Pessall, J.K. Hulm, Physics 2 (1966) 311.
[2] N. Pessall, R.E. Gold, H.A. Johansen, J. Phys. Chem. Solids 29 (1968) 19.
[3] E.J. Felten, J. Less-Common Metals 17 (1969) 207.
[4] R. Musenich, P. Fabbricatore, G. Gemme, et al., J. Alloys Comp. 209 (1994) 319.
[5] V. Buscaglia, C. Bottino, R. Musenich, et al., J. Alloys Comp. 226 (1995) 232.
[6] V. Buscaglia, R. Musenich, R. Parodi, W. Lengauer, W. Mayr, A. Tuissi, Proceedings of the Symposium 'Surface Performance of Titanium' ASM-TMS Materials Week '96, Cincinnati (OH), 7–10 October 1996.
[7] H. Holleck, Binäre und Ternäre Carbid- und Nitridsysteme der Übergangs-metalle, Gebrüder Borntraeger, Berlin-Stuttgart, 1984.
[8] E. Hornbogen, H. Warlimont, Metallkunde, 3rd ed., Springer-Verlag, Berlin, 1996.
[9] W. Lengauer, J. Bauer, M. Bohn, H. Wiesenberger, P. Ettmayer, Mikrochim. Acta 126 (1997) 279.
[10] W. Lengauer, P. Ettmayer, Monatsh. Chem. 117 (1986) 275.
[11] W. Lengauer, B. Tayenthal, R. Täubler, P. Ettmayer, in: Nichtmetalle in Metallen '92, DGM Informationsgesellschaft Verlag, Oberursel, 1992.
[12] W. Lengauer, J. Alloys Comp. 186 (1992) 293.
[13] A. Martinelli, Thesis, University of Genoa, 1995–96.
[14] C. Politis, G. Rejman, Jahresbericht 1977, Kernforschungszentrum Karlsruhe, 1978.